# 76. A-site acceptor doped $LaNbO_4$ thin film formation and structural investigation

**Kristina Bockute[1], Darius Virbukas[2], Giedrius Laukaitis[3]**
Physics Department, Kaunas University of Technology, Studentu 50, LT-51368 Kaunas, Lithuania
[3]Corresponding author
**E-mail:** [1]*kristina.bockute@ktu.lt*, [2]*darius.virbukas@ktu.lt*, [3]*giedrius.laukaitis@ktu.lt*

*(Received 7 October 2015; received in revised form 10 December 2015; accepted 21 December 2015)*

**Abstract.** In this paper, doped $La_{1-x}A_xNbO_4$ (A = Ca, Mg) thin films were formed using electron beam vapor deposition. The influence of the doping concentration of A site dopants (A = Ca, Mg) on the thin ceramics surface microstructure, morphology and electrical properties, including the charge carrier mobility and diffusion coefficient, was studied. It was found that the formed thin films are dense (>96 %) and have homogenous nanocrystalline structure composed of the tetragonal $LaNbO_4$ phase. The total conductivity of the formed thin films is in $10^{-3}$ S/cm range for Ca-doped $LaNbO_4$ and $10^{-4}$ S/cm range for Mg-doped $LaNbO_4$ at 800 °C under wet $H_2$ reducing atmosphere. The nature of protonic conduction was confirmed by the isotopic effect. The calculated $\Delta H_{mob,H}$ is 57 kJ/mol at 650 °C for the $La_{0.995}Ca_{0.005}NbO_4$ film, which total conductivity was highest in the present study ($9.52 \cdot 10^{-3}$ S/cm at 800 °C under wet $H_2$ reducing atmosphere). $\Delta H_{mob,H}$ increases steadily with increasing the dopants' concentration from 57 kJ/mol to 84 kJ/mol. The charge mobility decreases from $2.32 \times 10^{-5}$ cm$^2$/V·s to $6.25 \times 10^{-7}$ cm$^2$/V·s as the dopants' concentration increases at 650 °C.

**Keywords:** electron beam evaporation, nanocrystalline, proton conducting fuel cells (PCFC), doped lanthanum niobium oxide, $LaNbO_4$.

## 1. Introduction

During the past years, new proton conductive materials (as rare earth orthoniobates, e.g. lanthanum orthoniobate $LaNbO_4$) were thoroughly investigated as they show sufficient conductivity and good stability in different environment conditions. In addition, lanthanoides orthoniobates are ferroelastics, have excellent microwave dielectric properties, also they can be characterized as good luminescent materials [1-4]. $LaNbO_4$ exists in two polymorphs depending on the temperature: low temperature monoclinic Fergusonite type polymorph transforms to tetragonal Scheelite type structure at 450-550 °C [5-8]. This type of materials exhibits mixed protonic, native ionic and electronic conduction [9, 10]. Both low and high temperature polymorphs show protonic conduction, but dominant proton conductivity is up to 1000 °C, while at higher temperatures native ionic and electronic conduction takes place [11].

Netherless, the most common ceramic oxides with protonic conduction based on perovskite oxides ($ABO_3$) exhibit high protonic conductivity (~$10^{-2}$ S/cm), but they have poor chemical stability in $CO_2$ rich environment [12, 13], while lanthanum niobates are confirmed as stable material in $CO_2$ atmosphere [14]. Undoped lanthanum niobate shows the conductivity of $10^{-5}$ S/cm range [15] which is not acceptable for their use as the protonic conductors, therefore the acceptor doping is necessary to improve the protonic conductivity. To reach higher proton conductivity oxygen vacancies are proposed to be necessary. In $LaNbO_4$ oxygen vacancies are introduced by substituting La and/or Nb with lower valent cation. Dopant element has to be chosen by the ionic radius and the electronegativity. Usually $La^{3+}$ is substituted by the lower valent cations of $Ca^{2+}$, $Sr^{2+}$ and $Nb^{5+}$ by the $Ti^{4+}$, $Sn^{4+}$, or $Zr^{4+}$. The highest proton conductivity ~$10^{-3}$ S/cm is reached for $LaNbO_4$ doped with 1 % Ca [12]. The influence of Nb substitution and La and Nb site co-substitution to total conduction was studied also [1, 2, 5]. In all these works the findings are that neither Nb substitution nor La and Nb co-substitution showed higher proton conductivity compared to sole La substitution with Ca in $LaNbO_4$ [2]. The proton incorporation into the oxide matrix follows the same principle as for the perovskite oxides [16]. In wet atmosphere with the

presence of $H_2O$, water from the gas phase dissociates into hydroxide ion and a proton, the hydroxide ion fills an oxide ion vacancy and the proton form additional covalent bond with lattice oxygen [17]. Two hydroxide ions substitute oxide ions and two positively charged protonic defects are formed [15, 16, 18-21]. The concentration of protons could be increased by increasing the doping level of the aliovalent element. Lanthanum niobates may be formed using various preparation methods – conventional solid state reaction method [19], spray pyrolysis [22], sol-gel synthesis [9], coprecipitation [23], synthesis using freeze dried precursors [24] and etc. Several authors have investigated the influence of A site dopants (2, 5, 6, 8, 19, 25), B site dopants (21) or A and B site co-dopants (20) in bulk material, but only few papers present the investigation of the $LaNbO_4$ thin films [18, 25]. Each of the preparation method has its own advantages and disadvantages or limits, and with all these preparation methods, lanthanum niobate can exhibit largely varying properties. Lanthanum niobium ceramic oxides exhibit an order of magnitude lower proton conductivity compared to the best proton conductors of barium cerates. The conductivity of $LaNbO_4$ material can be improved by reducing the thickness of film and resistivity as well. In the present study, the thin films of lanthanum niobate were formed using one of the physical vapor deposition techniques - electron beam vapor deposition – as high density and surface homogeneity can be achieved with it. The influence of the doping concentration of A site dopants (A = Ca, Mg) on the thin ceramics surface microstructure, morphology and electrical properties, including the charge carrier mobility and diffusion coefficient, was investigated.

## 2. Experimental

Due to the different deposition rates and partial decomposition of the initial oxides lanthanum oxide $La_2O_3$ (99.9 % purity) and niobium pentoxide $Nb_2O_5$ (99.9 % purity) powders, both purchased from GoodFellow Ltd, were mixed in the molar ratio 1.3 $La_2O_3$ and 1 $Nb_2O_5$ as the elemental stoichiometry was achieved with such molar ratio in previous works [26]. To get $La_{1-x}Ca_xNbO_{4-\delta}$ and $La_{1-x}Mg_xNbO_{4-\delta}$ thin films, different concentration of calcium ($x = 0.005, 0.010, 0.015, 0.020, 0.025$) and magnesium ($x = 0.005, 0.010, 0.015, 0.020, 0.025$) was added to the powders mixture and mixed all together. The resulting powder was pressed to pellets and evaporated by electron beam physical vapor deposition (EB-PVD). Prior to deposition process the powder was preheated up to 1200 °C for 8 hours. Thin ceramic films were deposited on amorphous optical quartz ($SiO_2$), crystalline Fe-Ni-Cr alloy (Alloy 600) and high temperature resistant sapphire substrates to investigate their influence for the deposited thin films. To avoid any impurities on substrates, the substrates were carefully cleaned in the ultrasonic bath filled with pure acetone and in radio frequency Ar ions plasma in vacuum chamber before the deposition. The temperature of the substrates was raised to 600 °C at the time of deposition and the deposition rate was 2 Å/s. In order to get the surface homogeneity, the substrates were rotated at constant 8 rpm speed. The thickness of the formed thin films was 1.5 μm. The repeatability of the thin films having the same elemental composition was tested and confirmed by the statistical comparison of the elemental composition values and according to the standard deviations of the thin films produced during the 5 different depositions.

For the characterization of the formed thin films thickness profilometer Ambios XP-200 was employed. The density of the thin films was calculated from the measured films thickness, thin film mass and surface area. The crystallographic theoretical density of $LaNbO_4$ [27] was taken into the calculations. The surface morphology of the films was investigated with scanning electron microscope (SEM) Hitachi S-3400N and X-ray energy-dispersive spectroscope (EDS, Bruker X FLASH QUAD 5040, Bruker AXS GmbH) were employed to analyze the microstructure and the elemental composition of the formed films. X-ray diffraction (XRD, D8 Discover (Bruker AXS GmbH), Cu $K_{\alpha 1}$ $\lambda = 0.1540562$ nm radiation) was used to determine the crystallinity of the thin ceramics. The thin films were heated in-situ XRD chamber from 30 °C to 1000 °C and the XRD spectra were collected with a temperature step of 100 °C to investigate the thermal behavior of the doped $LaNbO_4$ thin films. The average grain size was calculated from the full width at half

maximum (FWHM) of the diffraction lines by using Topas 2P software according to Scherrer's relation [28].

The electrical characterization and impedance spectroscopy measurements were performed using Probostat® (NorECs AS) measurement cell in the frequency range from $10^{-1}$ to $10^6$ Hz and under $H_2$ reducing using pure hydrogen gas and $O_2$ oxidizing conditions using pure oxygen gas. The isotopic effect was measured using $5H_2$/He and $5D_2$/He gas mixture. The electrodes having the geometry 1×0.5 cm (L×B) were made of Pt ink and the sample was mounted in a Probostat® cell. Impedance spectroscopy was performed in parallel to film surface in the temperature range of 200 °C to 1200 °C with temperature step of 20 °C. The total conductivity $\sigma$ of the formed thin films was calculated from impedance spectra via total resistance $R_{total}$ using the relation $\sigma = L/AR_{total}$, where $L$ is the distance between electrodes and $A$ is the area of the electrode. The activation energy was calculated using Arrhenius law from obtained protonic conductivity plots at different measurement temperatures.

## 3. Experimental result and discussion

EDS analysis showed that the concentration of Ca and Mg dopants is slightly different than the initial dopant concentration in the prepared powder before the deposition. This change in the concentration occurred due to the different evaporation rate of the evaporated particles (Table 1). For the clarity the initial dopants' concentration will be used in the text.

**Table 1.** The dopants' concentration in $La_{1-x}A_xNbO_{4-\delta}$ thin films (A = Ca, Mg)

| Initial dopant concentration (expressed as x) in $La_{1-x}A_xNbO_{4-\delta}$ evaporated powder | Calcium concentration (expressed as x) in the formed thin films | Relative density, % | Magnesium concentration (expressed as x) in the formed thin films | Relative density, % |
|---|---|---|---|---|
| 0.005 | 0.007 | 96.8 % | 0.0047 | 97.1 % |
| 0.010 | 0.012 | 97.1 % | 0.0095 | 96.6 % |
| 0.015 | 0.018 | 97.2 % | 0.013 | 96.9 % |
| 0.020 | 0.022 | 96.9 % | 0.017 | 96.2 % |
| 0.025 | 0.026 | 97.1 % | 0.023 | 96.4 % |

The evaporation by electron beam vapor deposition method allows getting the high density of the formed thin. The relative density of the undoped $LaNbO_4$ was 95.4 % and the average relative density was 97.02 % for the Ca-doped $LaNbO_4$ films and 96.64 % for the Mg-doped thin films. The dopants increased the density of the formed thin films though no tendency was observed when the concentration of the dopants was changed. Such densification of the doped thin films was observed in lanthanum niobium oxide doped with Ca as well and with other doping elements [5, 15].

The micrographs in Fig. 1 illustrate the cross-sectional views of the thin $LaNbO_4$ films doped with different concentration of Ca and Mg dopants respectively. The morphology of the thin films formed using e-beam technology can be described by a Structure – Zone model (SZM) [29] corresponding to Zone T and Zone 2. As the substrate temperature was kept at 600 °C, the surface mobility was high enough to form zone T, i.e. tightly packed fibrous grains with weak grain boundaries, and then transform to a full-density nanocolumnar morphology corresponding to Zone 2 [30]. As we can see from Fig. 1, the formed thin films are dense, without visible pores and cavities, and the same nanocolumnar growth is observed for all the samples.

It was reported [31, 32] that $LaNbO_4$ is a "line compound" with low tolerance of the deviation of nominal 1:1 La/Nb ratio forming the secondary phases of $La_3NbO_7$. In our case, the formed thin films exhibit phase pure $LaNbO_4$ after annealing at 1000 °C. The XRD measurements of the as-deposited thin films revealed that all the films were amorphous except the $La_{0.995}Ca_{0.005}NbO_4$ film which was crystalline consisted of tetragonal $LaNbO_4$ phase. In order to investigate the

thermal behavior of the thin films they were heated up to 1000 °C in the XRD chamber and the XRD spectra were collected with 100 °C temperature step (Fig. 2).

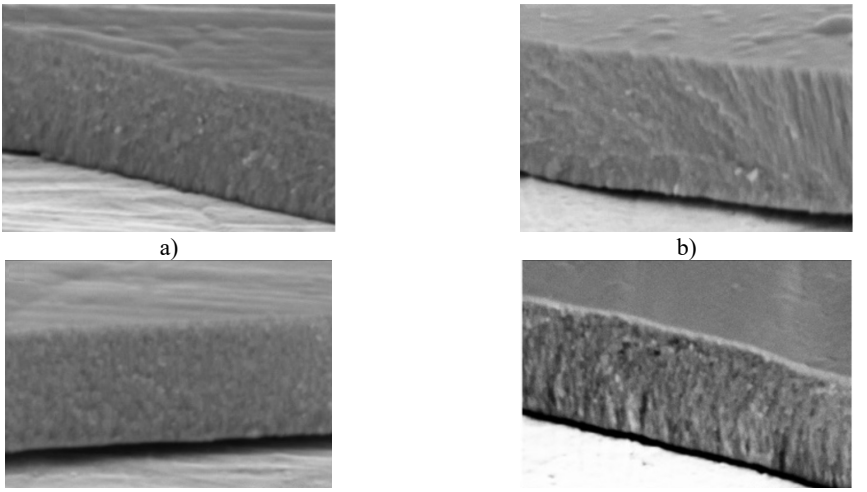

**Fig. 1.** SEM cross-sectional images of the formed thin $La_{1-x}Ca_xNbO_{4-\delta}$ films:
a) x = 0.005, c) x = 0.025; and thin $La_{1-x}Mg_xNbO_{4-\delta}$ films: b) x = 0.005, d) x = 0.025

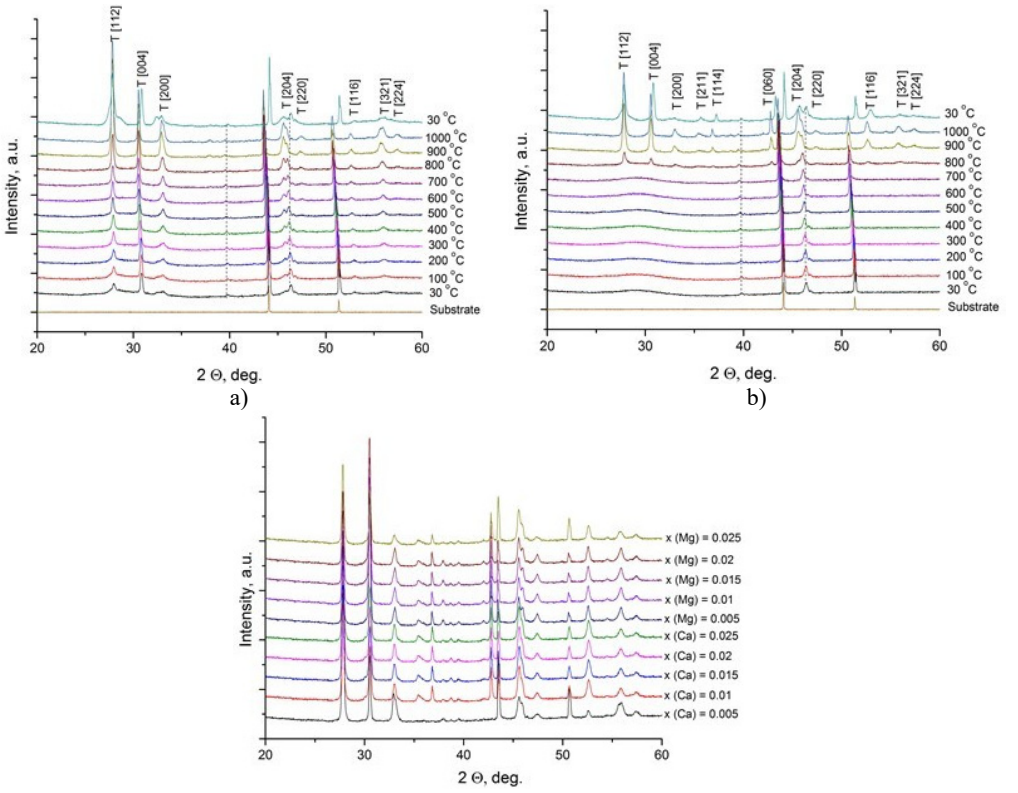


**Fig. 2.** X-Ray diffraction spectra of the doped-$LaNbO_4$ films: a) $La_{0.995}Ca_{0.005}NbO_4$ film, b) $La_{0.99}Ca_{0.01}NbO_4$ film, c) $La_{1-x}A_xNbO_{4-\delta}$ (A = Ca, Mg) films after the annealing at 1000 °C. Dashed lines represent the XRD peaks of the XRD heater

The crystalline $La_{0.995}Ca_{0.005}NbO_4$ film retained the tetragonal structure. All the other thin films crystallized from the amorphous phase to tetragonal phase at 800 °C. The formed thin films retained their tetragonal structure after the annealing. According to the relative intensity of the XRD peaks, no significant crystallographic texture can be found in the thin films. The size of the doped-$LaNbO_4$ crystallites was found to increase by increasing the concentration of the dopants (Fig. 3).

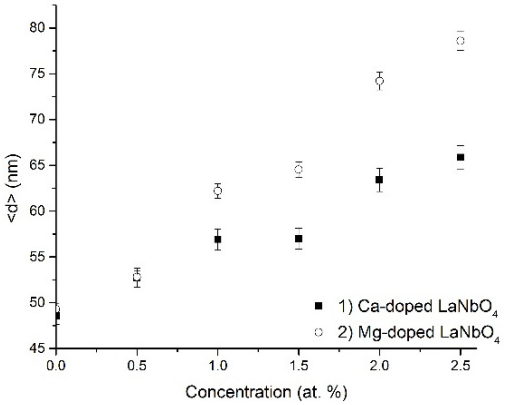


**Fig. 3.** Relationship between grain size and dopants' concentration in thin $La_{1-x}A_xNbO_{4-\delta}$ (A = Ca, Mg) films: 1) Ca-doped thin films, 2) Mg-doped thin films

It was observed from our previous works and other authors' works [25, 33, 34] that lanthanum niobium oxides have a tendency to form nanocrystalline phase when evaporating by electron beam vapor deposition method.

Fig. 4 presents an example from measured impedance spectroscopy showing the Niquist plot of data measured at 560 °C and 600 °C in wet $H_2$ atmosphere. This sweep was fitted according to the equivalent circuit consisting to one RC element. By increasing the temperature the total resistance of the thin film decreases.

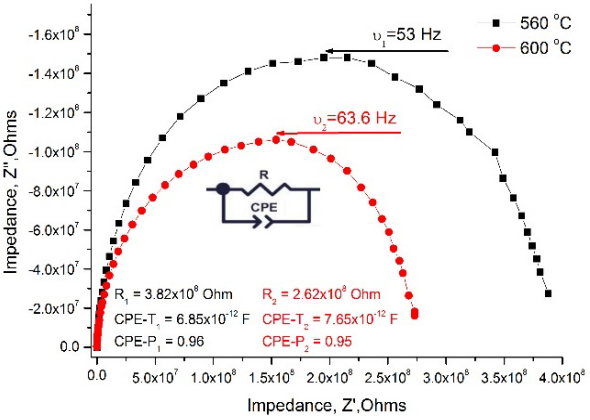


**Fig. 4.** Nyquist plot measured across the $La_{0.995}Ca_{0.005}NbO_4$ thin film under wet hydrogen atmosphere

It is not possible to distinguish the grains resistance from the impedance spectra as the nanocrystalline structure of the thin films was formed, therefore the total conductivity data is presented in the Table 2. It is seen that the size of the crystallites and the dopants' concentration has the influence on the total conductivity of the thin films. The total conductivity has a tendency to decrease when the size of the crystallites increases. The highest conductivity achieved is for the $La_{0.995}Ca_{0.005}NbO_4$ film and reaches $9.52\times10^{-3}$ S/cm at 800 °C under wet $H_2$ reducing atmosphere.

**Table 2.** The total conductivity of $La_{1-x}A_xNbO_{4-\delta}$ thin films (A = Ca, Mg) at 800 °C under wet $H_2$ and wet $O_2$ conditions

| Concentration of the dopants in $La_{1-x}A_xNbO_{4-\delta}$ thin films (A = Ca, Mg) | Conductivity under wet $H_2$, S/cm | | Conductivity under wet $O_2$, S/cm | |
|---|---|---|---|---|
| | Calcium dopant | Magnesium dopant | Calcium dopant | Magnesium dopant |
| x = 0.005 | $9.52\times\times10^{-3}$ | $2.67\times10^{-5}$ | $1.43\times10^{-5}$ | $6.42\times10^{-6}$ |
| x = 0.01 | $4.96\times10^{-4}$ | $2.82\times10^{-5}$ | $3.41\times10^{-5}$ | $1.10\times10^{-6}$ |
| x = 0.015 | $3.95\times10^{-4}$ | $6.11\times10^{-4}$ | $2.23\times10^{-5}$ | $2.28\times10^{-5}$ |
| x = 0.02 | $1.96\times10^{-4}$ | $1.18\times10^{-5}$ | $8.51\times10^{-5}$ | $3.10\times10^{-6}$ |
| x = 0.025 | $2.57\times10^{-4}$ | $1.09\times10^{-5}$ | $6.28\times10^{-5}$ | $2.52\times10^{-6}$ |

The conductivity is in the same order of magnitude as reported in the other works with doped lanthanum niobates [2, 4, 6, 8, 18, 19, 25]. The values of total conductivity of Mg-doped thin $LaNbO_4$ films are an order of magnitude lower than in Ca-doped $LaNbO_4$ [6, 35]. This tendency can be explained by the mismatch of ionic radius: ionic radius of Ca (1.26 Å) is more similar to ionic radius of La (1.3 Å) than ionic radius of Mg (1.06 Å), therefore doping with Ca is energetically more favorable and causes higher proton mobility [36].

The nature of protonic conduction was confirmed by the isotopic effect (Fig. 5), which assumes that the preexponential factor (A) is inversely proportional to the square root of the mass of isotopes: $A_H: A_D = 1{:}1/\sqrt{2} \approx 1.414$. This isotopic shift is in almost the whole temperature range and it becomes smaller at high temperature. Such behavior indicates that the conduction is mainly protonic for the samples under wet conditions.

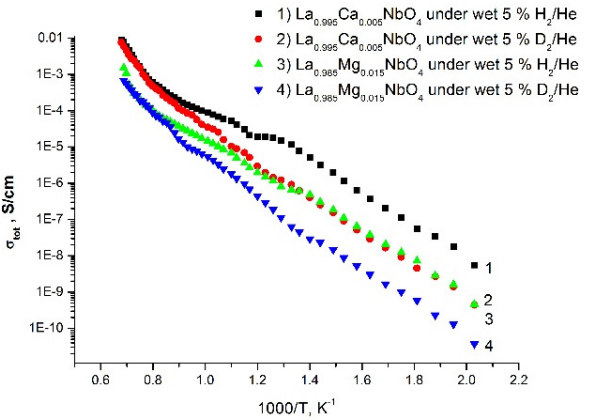


**Fig. 5.** Total conductivity as a function of inverse absolute temperature for $La_{0.995}Ca_{0.005}NbO_4$ thin film and $La_{0.985}Mg_{0.085}NbO_4$ thin film under wet 5 % $H_2$/He and wet 5 % $D_2$/He

The microstructure of the formed thin films has an influence on the diffusion coefficient and, thus, the charge mobility. As H. L. Tuller [37] and J. Maier [38] suggested the decrease in grain size in a material could lead to an increase of the total conductivity due to the grain boundaries effect. For nanocrystalline thin $La_{1-x}A_xNbO_{4-\delta}$ (A = Ca, Mg) films the segregation of the dopants to the grain boundaries could affect the charge concentration and charge mobility along the grain boundaries, therefore influencing the increase of the grain boundaries density. This increase could improve charge transport properties compared to polycrystalline materials with relatively large grain size. Protons migrate by activated diffusion, and the mobility, $u_H$, can be expressed according to an Arrhenius-type expression [36]:

$$u_H = u_{0,H}\frac{1}{T}\exp\left(-\frac{\Delta H_{mob,H}}{RT}\right), \quad (1)$$

where $u_H$ and $\Delta H_{mob,H}$ are the pre-exponential term and activation enthalpy of mobility of protons respectively. R. Haugsrud and T. Norby [17] obtained the activation enthalpy ($\Delta H_{mob,H}$) and pre-exponential term ($u_{0,H}$) respectively 55 kJ/mol and 35 $cm^2$ K/V s. According to the [17, 36] model, where $\sigma = z_i F u_i c_i$ and assuming that the concentration of the charge carriers at the same temperature is equal, and then the conductivity is dependent on the charge mobility $\sigma \in u_i$. The charge carriers' mobility was modeled from the Ca-doped thin $LaNbO_4$ film data as these films exhibit higher conductivity. $\Delta H_{mob,H}$ was calculated as a function of a temperature from $\Delta H_{mob,H} = RT\ln\sigma_{tot}$.

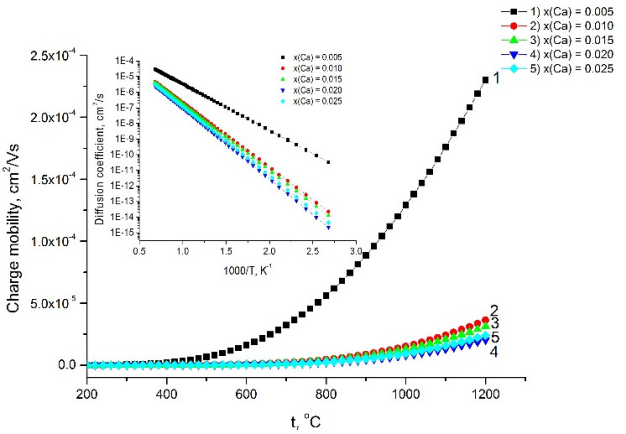


**Fig. 6.** Relationship between the charge mobility and the temperature. The inset presents the diffusion coefficient versus the temperature

The calculated $\Delta H_{mob,H}$ increases gradually with increasing the dopants' concentration, because Ca-doped $LaNbO_4$ is more distorted from the relative symmetrical structure of undoped $LaNbO_4$. $\Delta H_{mob,H}$ increases from 57 kJ/mol for the $La_{0.995}Ca_{0.005}NbO_4$ film to 84 kJ/mol for $La_{0.975}Ca_{0.025}NbO_4$ film at 650 °C temperature. The charge mobility depends on the conductivity and decreases from $2.32\times10^{-5}$ $cm^2$/V s to $6.25\times10^{-7}$ $cm^2$/V s as the dopants' concentration increase (Fig. 6). The inset of the Fig. 6 shows the diffusion coefficient calculated according to the $D_i = u_i\, RT/z_i F$.

## 4. Conclusions

Thin $La_{1-x}Ca_xNbO_{4-\delta}$ and $La_{1-x}Mg_xNbO_{4-\delta}$ films were formed using electron beam vapor deposition. The formed films are dense (>96 %) and have homogenous nanocrystalline structure. XRD revealed that the thin films are composed of the tetragonal $LaNbO_4$ after the annealing to 1000 °C. The size of the doped-$LaNbO_4$ crystallites increases by increasing the concentration of the dopants. The nature of protonic conduction was confirmed by the isotopic effect and the total conductivity is in $10^{-3}$ S/cm range for Ca-doped $LaNbO_4$ and $10^{-4}$ S/cm range for Mg-doped $LaNbO_4$ at 800 °C under wet $H_2$ reducing atmosphere. The calculated $\Delta H_{mob,H}$ is 57 kJ/mol at 650 °C for the $La_{0.995}Ca_{0.005}NbO_4$ film, which total conductivity was highest in the present study ($9.52\times10^{-3}$ S/cm at 800 °C under wet $H_2$ reducing atmosphere). $\Delta H_{mob,H}$ increases steadily with increasing the dopants' concentration from 57 kJ/mol to 84 kJ/mol. The charge mobility decreases from $2.32\times10^{-5}$ $cm^2$/V s to $6.25\times10^{-7}$ $cm^2$/V s as the dopants' concentration increases at 650 °C.

## References

**[1]** **Fisher E. S.** Elastic moduli and acoustic symmetry of ferroelastic $LaNbO_4$ and BiVO4. Journal of Physics: Condensed Matter, Vol. 1, 1989, p. 2875-2890.

**[2]** **Lin B., Wang S., Liu X., Meng G.** Stable proton-conducting Ca-doped LaNbO4 thin electrolyte-based protonic ceramic membrane fuel cells by in situ screen printing. Journal of Alloys and Compounds, Vol. 478, Issues 1-2, 2009, p. 355-357.

**[3]** **Huang J., Zhou L., Liang Z., Gong F., Han J., Wang R.** Promising red phosphors $LaNbO_4:Eu^{3+}$, $Bi^{3+}$ for LED solid-state lighting application. Journal of Rare Earths, Vol. 28, Issue 3, 2010, p. 356-360.

**[4]** **Magrasó A., Fontaine M.-L., Larring Y., Bredesen R., Syvertsen G. E., Lein H. L., Grande T., Huse M., Strandbakke R., Haugsrud R., Norby T.** Development of proton conducting SOFCs based on LaNbO4 electrolyte – status in Norway. Fuel Cells, Vol. 11, Issue 1, 2011, p. 17-25.

**[5]** **Fontaine M.-L., Larring Y., Hausgrud R., Norby T., Wiink K., Bredesen R.** Novel high temperature proton conducting fuel cells: production of La0.995Sr0.005NbO4−δ electrolyte thin films and compatible cathode architectures. Journal of Power Sources, Vol. 188, Issue 1, 2009, p. 106-113.

**[6]** **Haugsrud R., Norby T.** Proton conduction in rare-earth ortho-niobates and ortho-tantalates. Nature Materials, Vol. 5, 2006, p. 193-196.

**[7]** **Mokkelbost T., Lea Lein H., Erik Vullum P., Holmestad R., Grande T., Einarsrud M.-A.** Thermal and mechanical properties of LaNbO4-based ceramics. Ceramics International, Vol. 35, 2009, p. 2877-2883.

**[8]** **Malavasi L., Ritter C., Chiodelli G.** Investigation of the high temperature structural behavior of $La_{0.99}Ca_{0.01}NbO_4$ proton conducting material. Journal of Alloys and Compounds, Vol. 475, 2009, p. 42-45.

**[9]** **Hsiao Y. J., Fang T. H., Chang Y. S., Chang Y. H., Liu C. H., Ji L. W., Jywe W. Y.** Structure and luminescent properties of $LaNbO_4$ synthesized by sol-gel process. Journal of Luminescence, Vol. 126, 2007, p. 866-870.

**[10]** **Gupta U. N., Pradhan S., Muthurajan H., Kumar H. H., Kharat D. K., Ravi V.** A co-precipitation technique of preparing $LaNbO_4$ powders. Journal of the American Ceramic Society, Vol. 90, 2007, p. 2661-2663.

**[11]** **Prytz O., Tafto J.** Accurate determination of domain boundary orientation in $LaNbO_4$. Acta Materiala, Vol. 53, 2005, p. 297-302.

**[12]** **Demin A. K., Tsiakaras P. E., Sobyanin V. A., Hramova S. Y.** Thermodynamic analysis of a methane fed SOFC system based on a protonic conductor. Solid State Ionics, Vol. 153, 2002, p. 555-560.

**[13]** **Iwahara H., Esaka T., Uchida H., Maeda N.** Proton conduction in sintered oxides and its application to steam electrolysis for hydrogen production. Solid State Ionics, Vol. 3, Issue 4, 1981, p. 359-363.

**[14]** **Magrasó A., Fontaine M.-L., Bredesen R., Haugsrud R., Norby T.** Cathode compatibility, operation, and stability of $LaNbO_4$-based proton conducting fuel cells. Solid State Ionics, Vol. 262, 2014, p. 382-387.

**[15]** **Mokkelbost T., Kaus I., Haugsrud R., Norby T., Grande T., Einarsrud M.-A** High-temperature proton-conducting lanthanum ortho-niobate-based materials. Part 2: sintering properties and solubility of alkaline earth oxides. Journal of American Ceramic Society, Vol. 91, 2008, p. 879-886.

**[16]** **Kreuer K. D.** Proton-conducting oxides. Annual Review of Materials Research, Vol. 33, 2003, p. 333-359.

**[17]** **Haugsrud R., Norby T.** High-temperature proton conductivity in acceptor-doped $LaNbO_4$. Solid State Ionics, Vol. 177, 2006, p. 1129-1135.

**[18]** **Cavallaro A., Solís C., Garcia P. R., Ballesteros B., Serra J. M., Santiso J. L.** Epitaxial films of the proton-conducting Ca-doped $LaNbO_4$ material and a study of their charge transport properties. Solid State Ionics, Vol. 216, 2012, p. 25-30.

**[19]** **Bi Z., Peña-Martínez J., Kim J.-H., Bridges C. A., Huq A., Hodges J. P., Paranthaman M. P.** Effect of Ca doping on the electrical conductivity of the high temperature proton conductor $LaNbO_4$, International Journal of Hydrogen Energy, Vol. 37, 2012, p. 12751-12759.

**[20]** **Ivanova M., Ricote S., Meulenberg W. A., Haugsrud R., Ziegner M.** Effects of A- and B-site (co-) acceptor doping on the structure and proton conductivity of $LaNbO_4$. Solid State Ionics, Vol. 213, 2012, p. 45-52.

**[21]** **Brandão A. D., Gracio J., Mather G. C., Kharton V. V., Fagg D. P.** B-site substitutions in $LaNb_{1-x}M_xO_{4-\delta}$ materials in the search for potential proton conductors. Journal of Solid State Chemistry, Vol. 184, Issue 4, 2011, p. 863-870.

**[22]** **Xing W., Syvertsen G. E., Grande T., Li Z., Haugsrud R.** Hydrogen permeation, transport properties and microstructure of Ca-doped $LaNbO_4$ and $LaNb_3O_9$ composites. Journal of Membrane Science, Vol. 415, Issue 416, 2012, p. 878-885.

**[23]** **Zhang Z., Zhou L., Hu Y., Jiang L.** Preparation and characterization of $Al_2O_3$-$LaNbO_4$ composites. Scripta Materialia, Vol. 47, 2002, p. 637-641.

**[24]** **Amsif M., Marrero-López D., Ruiz-Morales J.C., Savvin S., Núñez P.** Low temperature sintering of $LaNbO_4$ proton conductors from freeze-dried precursors. Journal of the European Ceramic Society, Vol. 32, 2012, p. 1235-1244.

**[25]** **Bozza F., Schafbauer W., Meulenberg W. A., Bonanos N.** Characterization of $La_{0.995}Ca_{0.005}NbO_4$/Ni anode functional layer by electrophoretic deposition in a $La_{0.995}Ca_{0.005}NbO_4$ electrolyte based PCFC. International Journal of Hydrogen Energy, Vol. 37, 2012, p. 8027-8032.

**[26]** **Bočkutė K., Laukaitis G., Milčius D.** The properties of nonstoichiometric lanthanum niobium oxide thin films formed using an e-beam deposition technique. Surface and Coatings Technology, Vol. 214, 2013, p. 97-100.

**[27]** **Tsunekawa S., Kamiyama T., Sasaki K., Asano H., Fukuda T.** Precise structure analysis by neutron diffraction for $RNbO_4$ and distortion of $NbO_4$ tetrahedra. Acta Crystallographica, Vol. A49, 1993, p. 595-600.

**[28]** **Birks L. S., Friedman H.** Particle size determination from X-Ray line broadening. Journal of Applied Physics, Vol. 17, Issue 8, 1946, p. 687-692.

**[29]** **Grovenor C. R. M., Hetzell H. T. G., Smith D. A.** The development of grain structure during growth of metallic films. Acta Metallurgica, Vol. 32, Issue 5, 1984, p. 773-781.

**[30]** **Peter M. M.** Handbook of Deposition Technologies for Films and Coatings. 3rd Ed., Oxford, 2010.

**[31]** **Magrasó A., Fontaine M.-L.** Investigation of compatible anode systems for $LaNbO_4$-based electrolyte in novel proton conducting solid oxide fuel cells. Journal of Power Sources, Vol. 196, Issue 23, 2011, p. 10183-10190.

**[32]** **Syvertsen G. E., Magrasó A., Haugsrud R., Einarsrud M.-A., Grande T.** The effect of cation non-stoichiometry in $LaNbO_4$ materials. International Journal of Hydrogen Energy, Vol. 37, 2012, p. 8017-8026.

**[33]** **Yang C., Fan H., Qiu S., Xi Y., Fu Y.** Microstructure and dielectric properties of $La_2O_3$ films prepared by ion beam assistant electron-beam evaporation. Journal of Non-Crystalline Solids, Vol. 355, Issue 1, 2009, p. 33-37.

**[34]** **Kim Y., Miyauchi K., Ohmi S., Tsutsui K., Iwai H.** Electrical properties of vacuum annealed $La_2O_3$ thin films grown by E-beam evaporation. Microelectronics Journal, Vol. 36, Issue 1, 2005, p. 41-49.

**[35]** **Mielewczyk-Gryn A., Gdula K., Molin S., Jasinski P., Kusz B., Gazda M.** Structure and electrical properties of ceramic proton conductors obtained with molten-salt and solid-state synthesis methods. Journal of Non-Crystalline Solids, Vol. 356, 2010, p. 1976-1979.

**[36]** **Fjeld H., Toyoura K., Haugsrud R., Norby T.** Proton mobility through a second order phase transition: theoretical and experimental study of $LaNbO_4$. Physical Chemistry Chemical Physics, Vol. 35, 2010, p. 10313-10319.

**[37]** **Tuller H. L.** Solid state electrochemical systems-opportunities for nanofabricated or nanostructured materials. Journal of Electroceramics, Vol. 1, Issue 3, 1997, p. 211-218.

**[38]** **Maier J.** Nano-sized mixed conductors (Aspects of nano-ionics. Part 3). Solid State Ionics, Vol. 148, Issues 3-4, 2002, p. 367-374.